

CONCEPTUAL DESIGN STUDY ON LOW BOOM LH₂ SUPERSONIC TRANSPORT - CONSIDERING CLIMATE CHANGE IMPACT -

Tatsunori YUHARA*

***7-3-1 Hongo, Bunkyo-ku, Tokyo, 113-8656, Japan**

129446954@mail.ecc.u-tokyo.ac.jp

Keywords: *Conceptual design, Supersonic aircraft, Sonic boom, Climate change Impact*

Abstract

As new fuel of next generation supersonic transport, the author proposes liquid hydrogen (LH₂). The reason is that LH₂ fuel has a potential to greatly reduce weight of aircraft. However, it was reported by IPCC that H₂O emission in the stratosphere could have significant impact on global warming. The purpose of this paper is to conduct conceptual design of LH₂ supersonic transport by using the author's conceptual design procedure incorporated with climate functions which outputs global mean surface temperature change (ΔT) as a metric of climate change impact. Multi objective optimization has been conducted under several constrained conditions including low speed aerodynamics, high speed stability and sonic boom metric. Scatter Plot Matrix (SPM) quantitatively reveals correlations between variables and objective functions on the pareto solutions. Especially, it is found that there is a tradeoff relationship between ΔT and lift to drag ratio (L/D). Self-Organizing Map (SOM) reveals relationships between leading and trailing edge swept angles (LLE1, LLE2, LTE1, LTE2) and L/D . An optimized population has been selected among the pareto solutions. Compared with an initial model, improvements have been confirmed.

1 Introduction

Many projects have made efforts to realize commercial supersonic transports. These trials have revealed many barriers for the successful completion of various necessary project goals,

related to supersonic cruise efficiency, sonic boom annoyance, economic viability and also the development of solutions for avoiding environmental problems. The author has proposed LH₂ as fuel of next generation supersonic transport [1]. The reason is that LH₂ has a potential to reduce weight of an aircraft greatly because of the higher energy density. Table 1 lists the property of LH₂ and kerosene. However, it was reported by IPCC that H₂O, i.e., water vapor emission in the stratosphere could have significant impact on global warming [2]. It can be a difficult problem for aircraft fueled by LH₂.

The purpose of this paper is to conduct conceptual design of LH₂ supersonic transport by using the author's conceptual design procedure incorporated with climate functions [3] which outputs global mean surface temperature change (ΔT) as a metric of climate change impact. Multi objective optimization will be conducted under several constrained conditions including low speed aerodynamics, high speed stability and sonic boom metric. Then, data mining techniques extract information of optimized solutions.

2 Climate impact by supersonic aircraft

2.1 Overview

Air traffic is growing with significant speed year by year. It is expected to grow further in the future. It is well known that global warming is induced by gases and non-gas contributors. Carbon dioxide (CO₂), water vapor (H₂O), methane (CH₄) and ozone (O₃) are the major

greenhouse gases. Aerosol and contrails are also the major non-gas contributors. In order to quantify contribution to global warming, radiative forcing indices have been used, which is defined as the change in average net radiation in watt per square meter. In simple terms, radiative forcing index expresses the earth's energy budget. Carbon dioxide has stronger positive radiative forcing, i.e., increases the earth's energy so as to warm the atmosphere. The reason is the long residence time of carbon dioxide in the order of year. In addition, the impact of carbon dioxide is independent on latitude and altitude. In 1999, it was reported that water vapor at a higher altitude, in the stratosphere, could have strong positive radiative forcing [2]. In the troposphere, water vapor can fall on the earth's surface by rain. However, water vapor stays for a longer time in the stratosphere where there is little convection and mixing and no rain. Methane and ozone also have positive radiative forcing.

2.2 Aircraft emission

Conventional kerosene-type jet fuel consists preliminarily of hydrocarbon (C_mH_n). Burning jet fuel with air, which is composed mainly of nitrogen (N₂) and oxygen (O₂) in the stratosphere as well as in the troposphere, produces carbon dioxide, water and nitrogen oxides (NO_x). Carbon dioxide and water vapor directly affects global warming as previously mentioned. On the other hand, nitrogen oxides indirectly contribute to global warming by producing or depleting ozone. Nitrogen oxides at a high altitude are decomposed by ultraviolet radiation. The reaction speed varies with altitude. Thus, whether nitrogen oxides produces or depletes ozone is determined by altitude. Generally speaking, ozone is produced in the troposphere, but depleted in the stratosphere. The production of ozone decreases the amount of existing methane by producing OH radicals.

2.3 Climate function

Supersonic aircraft will fly in the stratosphere for better cruise efficiency. An investigation for

a supersonic transport (250pax, M2.0, cruise level 54 and 64 kft) has about 6 times larger impact on climate than a comparable subsonic transport [4]. Thus, it is required to estimate the effect quantitatively in the conceptual design phase of a supersonic transport. In order to predict the climate change impact by aircraft emission with high fidelity, complicated physics models should be applied. The state-of-art forecasting technology utilizes large-scale computing. However, it is not suitable for conceptual design phase of aircraft because of the computational time. In 2009, Grewe proposed climate functions for the use in the pre-design of supersonic business jet [3]. The climate functions are the simplified expressions of a climate chemistry model AirClim which was developed and validated in 2008 [4]. As shown in following equations, global mean climate change impact by each greenhouse gases is expressed in near surface temperature change (ΔT [mK]).

$$\Delta T = \Delta T_{CO_2} + \Delta T_{H_2O} + \Delta T_{O_3} + \Delta T_{CH_4} \quad (1)$$

$$\Delta T_{CO_2} = 1.65 \times 10^{-10} \times FC \quad (2)$$

$$\Delta T_{H_2O} = [-626 \times \log(P_{CA}) + 1449] \times \frac{FC}{FC_{SCENIC}} \quad (3)$$

$$\Delta T_{O_3} = [-53.4492836 + \sqrt{68730.2188 \times \log(P_{CA}) - 116758.68}] \times \frac{FC \times EINOx}{FC_{SCENIC} \times EINOx_{SCENIC}} \quad (4)$$

$$\Delta T_{CH_4} = [-109.328255 \times \log(P_{CA})^2 + 462.227 \times \log(P_{CA}) - 504.7347] \times \frac{FC \times EINOx}{FC_{SCENIC} \times EINOx_{SCENIC}} \quad (5)$$

Where PCA: Pressure at cruise altitude [hPa]
 FC: Fuel consumption [kg]
 EINO_x: Emission index of NO_x [g/kg]

Grewe obtained these expressions by fitting the result of the AirClim as shown in Fig. 1. This result shows temperature changes in 2100 calculated under a condition where supersonic

aircraft enter into service in 2015 and full fleet available in 2050. The AirClim can calculate the temperature change for regions which are divided by latitude and altitude. In obtaining the above expressions, the latitude dependence is removed by weighting profiles, where it is assumed that 40% of the emissions take place at mid-latitudes (22.5 degree N to 60 degree N) and the rest equally distributed.

2.4 Application to LH₂

The climate functions have been developed for conventional jet-fuel. In applying them to LH₂ fuel, simple modifications have been made.

The average chemical formula for conventional kerosene-type jet fuel is C₁₂H₂₃. Completely burning 1.00 kg of C₁₂H₂₃ produces 3.15 kg of CO₂ and 1.24 kg of H₂O. On the other hand, burning 1.00 kg of LH₂ produces 0.00 g of CO₂ and 8.94 kg of H₂O.

Thus, the production of H₂O by burning LH₂ can be 7.21 times more than that by burning C₁₂H₂₃. Therefore, the climate functions can be changed according to this factor.

NO_x emission, i.e., thermal NO_x, also differs between jet-fuel and LH₂ fuel. NO_x emission mainly depends on flame temperature in combustion chamber. The flammable range of hydrogen is broader than that of kerosene so that the flame temperature can be suppressed. Thus it will lead to NO_x reduction [5].

2.5 Characteristics

The characteristics of the climate change impacts by kerosene fuel and LH₂ fuel have been compared here.

Fig. 2 (a) and (b) show contour maps of ΔT varied by altitude (*ALT*) and *EINO_x*. The values have been non-dimensionalized by the max values. Both *ALT* dependence and *EINO_x* dependence can be seen in case of kerosene fuel while only *ALT* dependence can be confirmed in case of LH₂. The reason is that ΔT by H₂O emission depends only on *ALT* as shown in Eq. (3) and the contribution of H₂O emission to ΔT is larger than the other contribution in case of LH₂.

3 Conceptual design procedure

3.1 Overview

Aircraft design is typically divided into 3 steps, conceptual design, preliminary design and detailed design. Conceptual design is a work to evaluate feasibility of a new concept. Preliminary design raises the feasibility by considering the concept carefully. Detail design is a pre-step to manufacture the concept model actually. The roles of conceptual design are to consider every aspect of the possibility and to extend the knowledge. Thus, conceptual design tools should produce results rapidly and broadly.

A conceptual design procedure for supersonic aircraft has been developed by the author as shown in Fig. 3. In order to produce results rapidly, linear theory based aerodynamics estimation tools are utilized. An empirical method is adopted in weight estimation. Table 2 shows the tools utilized in this paper. The climate functions are also included in the procedure. The routines are automated by batch processing in order to apply to a parametric study tool e.g., Design Of Experiment (DOE). In this paper, Multi-Objective Genetic Algorithm (MOGA) [6] has been utilized to obtain a broad range of solutions.

3.2 Geometry generation

Fuselage shape is defined as a circular body. Non-Uniform Rational B-Spline (NURBS) determines the radii distributions.

Wing coordinates are given by WARP program [7] which calculates an optimum camber and twist distribution under a given planform. The program is based on Carlson's method [8].

3.3 Weight estimation

For structural component weight estimation, an empirical estimation method has been utilized. The equations are based on WAATS [9]. The coefficients have been updated by using weight data of previous SST projects [10-13].

For fuel weight estimation, the fuel fraction method has been utilized [14].

3.4 Aerodynamics estimation

FRICION calculates viscous drag and pressure drag by separation of an aircraft by using flat plate analogy and form factor method [15].

PANAIR estimates pressure drag and longitudinal moments by using three-dimensional panel method [16].

3.5 Sonic boom reduction

In general, an aircraft cruising supersonic speed generates pressure wave called sonic boom. The reason of the loud noise is the shape of N wave. However, appropriate modification of aircraft's shape can prevent sonic boom shape from N wave. Seebass-George-Darden method (SGD method) gives an indication for the modification [17-18].

Figure 4 explains the concept of the SGD method. According to a flight condition, the method gives an F-function (near-field pressure signature) which leads to a far-field pressure signature of non N wave. The method can generate two types, flat-top type sonic boom which has minimum overpressure and ramp-type sonic boom which has minimum shock. The F-function can be converted into an equivalent area distribution which is referred to as a 'target equivalent area distribution' in this paper. Thus, when an aircraft's equivalent area distribution fits closely with a target equivalent area distribution, the aircraft's sonic boom can be shaped. The above routines are packaged in SEEB program.

Figure 5 shows an equivalent area distribution which includes two elements, due to volume and lift. Equivalent area due to volume is cross sectional area cut by Mach plane which has been obtained by D2500 program [19]. Equivalent area due to lift is obtained by integrating lift distribution which has been obtained by PANAIR. ΔA_E is the difference of the equivalent areas between the total (volume + lift) and the target. Note that ΔA_E is the root mean square and non-dimensionalized by using a reference length.

3.6 Application to LH₂ fuel

In designing a LH₂ supersonic transport, some assumptions have been made in weight estimation.

LH₂ tank has been assumed to be installed in fuselage. The tank should be designed to endure high pressure and low temperature. The shape becomes cylindrical naturally. Thus, the tank weight has been added to structural weight and estimated to be 24% of fuel weight [20]. LH₂ fuel supply system has been assumed to have more components than that of jet-fuel, e.g. gas generator. Thus, the LH₂ fuel supply system weight has been estimated to be 85 % heavier than conventional jet fuel system [20]. Specific fuel consumption is one of the most critical parameters in aircraft design. The specific fuel consumption of LH₂ has been assumed to be one-third of that of jet-fuel because of the higher energy density [20].

4 Optimization and data mining

4.1 Overview

Trade-off relationships exist among aircraft performances. Recently, multi-objective optimization based on evolutionary algorithm has been applied to aircraft design in order to obtain pareto solutions in a single run. The evolutionary algorithm utilizes the way of biological evolution. Although the algorithm is a probabilistic approach and time-consuming method compared with a gradient-based algorithm, it can be a strong tool if appropriate settings are selected. The algorithm does not use any gradient information so that it is easy to implement and it can find out a global optimization point. In general, the algorithm requires a larger amount of calculation. Thus, data mining techniques have been tried for analyzing the many calculation results.

4.2 Multi-objective optimization method

In order to obtain pareto solutions, MOGA has been utilized [6]. In this paper, pareto ranking method has been adopted for the fitness

calculation. Blended crossover (BLX) has been employed for the crossover [21]. CHC has been incorporated for the generation model [22].

4.3 Data mining method

4.3.1 Scatter plot matrix

In order to see correlations between variables and objective functions quantitatively, Scatter Plot Matrix (SPM) has been utilized for the visualization [23]. In this paper, scatter plots are shown in upper triangular matrix and correlation coefficient in lower triangular matrix. See Fig. 9. As correlation coefficient approaches 1.0, it means strong correlation.

4.3.2 Self-organizing map

In order to cluster solutions by similarity, Self-Organizing Map (SOM) has been utilized [24]. The SOM is a type of artificial neural network that is trained using unsupervised learning to produce two-dimensional map from high-dimensional input data. In this paper, rectangle map composes of hexagon. See Fig. 10. Each hexagonal cell in the rectangle maps links by the position. When two maps are compared and the color pattern looks similar, it can be said that the two data has correlation. MATLAB SOMToolbox has been utilized for the implementation [25].

5 Conceptual design results

5.1 Overview

Conceptual design is a work to evaluate feasibility of a new concept. Specifically, the work includes comparing with an existing concept, considering every aspect of the new concept and extending the knowledge.

In this paper, mission requirements have been selected. Then, preliminary sizing has been implemented to build an initial model. The sizing results have been compared with a case of kerosene fuel. Last, MOGA, SPM and SOM have been executed for gaining the further knowledge.

5.2 Mission requirements

In 2007, NASA announced several goals that future supersonic transports should accomplish, including cruise emissions, airport noise and sonic boom criteria [26].

In this paper, following mission requirements have been selected according to the NASA's N+3 goal. The goal aims at relatively large supersonic transport. The sonic boom goal of 65-70 PLdB is so aggressive that it is necessary to take a measure. The quantitative goal of climate change impact is to be determined. However, efforts for reducing the change are made. *EINOx*, full fleet size and full fleet available year have been selected for calculating the climate functions according to ref. [3].

| | |
|--------------------------------|-----------------|
| Fuel: | LH ₂ |
| Configuration: | Tube-Wing |
| Cruise speed: | M1.6 |
| Passenger: | 100PAX |
| Range: | 6,000nm |
| Balanced Field Length: | 10,000ft |
| Landing Field Length: | 10,000ft |
| Sonic Boom: | 65-70 PLdB |
| Climate change impact: | TBD |
| <i>EINOx</i> : | 15 |
| Full fleet size: | 250 |
| Flights per aircraft and year: | 100 |
| Full fleet available: | in 2050 |

5.3 Preliminary sizing

Three requirements, i.e., second segment climb rate (SSC), landing field length (LFL) and balanced field length (BFL), give allowable region of takeoff wing loading (W/S) and thrust to weight ratio (T/W). The W/S and T/W has been selected to be 50 psf and 0.32 by assuming takeoff climb L/D of 6.0.

The wing planform has been selected to be a conventional swept wing. The fuselage volume has been set to be 58,000 ft³ including 26,500 ft³ of the tanks and 20,000 ft³ of the cabin. The fuselage shape has been tailored to meet a target equivalent area distribution.

Table 3 shows the specification and Fig. 6 show the planview.

5.4 Comparison with kerosene fuel

Three conditions have been set for the comparison: 1. Unify cabin volume to maintain passenger comfort. 2. Select W/S and altitude that minimize takeoff weight. 3. Tailor geometry for low sonic boom.

Table 3 shows the specification. LH_2 fuel can make the takeoff weight reduction of 30 %. However, the average surface temperature change of 2.37 mK is higher than that of kerosene. It is found that the global mean surface temperature change (ΔT) by H_2O emission dominates the total ΔT in case of LH_2 while that of O_3 dominates in case of kerosene.

5.5 Optimization and data mining

5.5.1 Conditions

Preliminary sizing has given an initial model. In order to search a broader range of solution space, MOGA has been executed. Some trials before optimization have indicated that L/D is potentially improved so that the fuel volume has been reduced and the fuselage volume has been also reduced from 58,000 ft³ to 55,000 ft³.

Table 4 shows the algorithm settings and the optimization conditions of MOGA. The generation of 30 and population of 100 have been set.

Nine design variables have been selected including aspect ratio (AR), kink position ($KINK$), leading and trailing edge swept angles ($LLE1$, $LLE2$, $LTE1$, $LTE2$), wing area ($AREA$), fuselage fineness ratio (FR) and cruise altitude (ALT). Fig. 7 and Table 5 show the design variables. FR indicates the ratio between fuselage length and diameter.

Three objective functions have been selected including takeoff weight (W_{TO}), lift to drag ratio (L/D) at cruise and average surface temperature change (ΔT or $DeIT$) as shown in Table 5.

Three constrained conditions have been set including takeoff-climb induced drag coefficient ($K@T/O$ or low speed aerodynamics condition), cruise static-margin ($\Delta X_{AC}@cruise$ or high speed stability condition) and equivalent area distribution difference (ΔA_E or sonic boom

condition) as shown in Table 6. Populations which survived the sonic boom condition can have shaped sonic boom signature with minor shape modification.

Some parameters have been set constant purposely, including fuselage volume, fuel tank volume (i.e., fuel weight), wing back-end position and T/W . The wing back-end position has been located at 90 % of the fuselage length. The reason is that extending lift distribution backward helps rear shock reduction of sonic boom. In addition, the fuel weight is set to be constant while maximizing L/D . Thus, it can be said that this optimization problem is a cruise-range maximization problem.

5.5.2 Results

Fig. 8 shows the pareto solutions. Note that some errors in aerodynamics calculation have been removed (the error occasionally happens in implementing PANAIR). A pareto ‘curved surface’ is observed.

Table 7 (a) and (b) show the average (AVE), the standard deviation (STDEV) and the coefficient of variation (rate between AVE and STDEV) of the non-pareto solutions and the pareto solutions. It is found that all variable values have been narrowed down when compared to the setting ranges. The reason is the three constrained conditions. Especially, the author’s previous work showed that minimizing ΔA_E narrows down ALT [1]. The low speed aerodynamics condition and high speed stability condition also limit wing planform geometry.

SPM and SOM analysis have been executed on the pareto solutions as shown in Fig. 9 and 10. Note that the information of these figures will be helpful only for the neighborhood of the pareto solutions.

Fig. 9 shows that AR and $FINE$ have relatively high correlation with W_{TO} . Thus, it can be said that modification of AR or $FINE$ will affect W_{TO} .

Fig. 9 also shows that ALT , L/D and ΔT have relatively high correlation with each other. Thus, a tradeoff relation can be seen between L/D and ΔT . The correlation between ΔT and ALT can be seen from Eq. (1-5). The correlation between ALT and L/D has been analyzed more detail by seeing correlation coefficients between

ALT and friction drag (C_{DF}), between ALT and induced drag (C_{DI}) and between ALT and C_L , i.e., 0.55, 0.96 and 0.98, respectively. There is an optimum C_L to maximize L/D . Sensitivity of cruise C_L to L/D is raised when the cruise C_L is apart from the optimum C_L . It is considered that the same situation occurs in this case .

Fig. 10 shows the other information of L/D . Cells which have higher L/D are located at the left lower in the maps. In that region, $LLE1$, $LLE2$, $LTE1$, $LTE2$ and ALT are also relatively high value. The relationship between ALT and L/D can be explained as follows. As ALT increases, cruise C_L comes closer to optimum C_L . Then, L/D also increases. The relationships between $LLE1$, $LLE2$, $LTE1$, $LTE2$ and L/D can be explained by using planform parameter which is defined as ratio between wing area and rectangular area as shown in Fig. 11. As $LLE1$, $LLE2$, $LTE1$ and $LTE2$ increase, planform parameter decreases. Higuchi showed that as the planform parameter decrease, supersonic lift dependent drag also decreases [27]. Then, L/D also increases.

A population whose L/D is relatively high value has been selected in the pareto solutions. Fig. 12 shows the planview and the equivalent area distribution. Table 8 shows the specification. Compared with the initial model, W_{TO} has improved by 10 %. L/D has also improved by 8 % so that Range has extended by 10 % while keeping the same level of ΔT .

6 Discussion

6.1 Climate change impact

In order to reduce absolute ΔT of LH₂ supersonic aircraft emission, one of the options is to reduce cruise altitude. However, the sonic boom condition narrows down the feasible range of cruise altitude. Another option is to reduce fuel consumption. However, there is a tradeoff relationship between L/D and ΔT . Therefore, there is a limitation for reducing absolute ΔT by changing airframe and altitude.

Conventional transports usually fly on great circles to minimize cruise range distance and also there is a latitude dependence of ΔT as

shown in Fig. 1. If the overconcentration of water vapor emission in the stratosphere would raise ΔT , distributing flight path could be an option.

6.2 Feasibility of LH₂ supersonic transport

MOGA has been conducted under several constrained conditions including low speed aerodynamics, high speed stability and sonic boom metric. Thus, it can be said that the survived populations are relatively practical.

For more practical solutions, the other constrained conditions should be added such as takeoff noise condition or structural condition. Increasing constrained conditions will raise the feasibility.

7 Conclusions

- LH₂ supersonic transport has been conceptually designed by using the author's conceptual design procedure incorporated with the climate functions which outputs global mean surface temperature change (ΔT) as a metric of climate change impact.
- Multi objective optimization has been conducted under several constrained conditions including low speed aerodynamics, high speed stability and sonic boom metric.
- Scatter Plot Matrix (SPM) reveals correlations between variables and objective functions on the pareto solutions. It is found that there is a tradeoff relationship between ΔT and lift to drag ratio (L/D). It is also found that there is a high correlation between altitude (ALT) and L/D and the dominant contributor is cruise C_L .
- Self-Organizing Map (SOM) reveals relationships between leading and trailing edge swept angles ($LLE1$, $LLE2$, $LTE1$, $LTE2$) and L/D .
- Among pareto solutions, an optimized population has been selected. Compared with an initial model, improvements have been confirmed.

Acknowledgement

The authors would like to thank Dr. Akira Murakami, Dr. Kenji Yoshida, Dr. Yoshikazu Makino, Mr. Shigeru Horinouchi and Dr. Keiichi Okai of JAXA for their advices.

This study was supported by Grant-in-Aid for JSPS research Fellows.

Copyright Statement

The authors confirm that they, and/or their company or organization, hold copyright on all of the original material included in this paper. The authors also confirm that they have obtained permission, from the copyright holder of any third party material included in this paper, to publish it as part of their paper. The authors confirm that they give permission, or have obtained permission from the copyright holder of this paper, for the publication and distribution of this paper as part of the ICAS2012 proceedings or as individual off-prints from the proceedings.

References

- [1] Yuhara, T. and Rinoie, K., "Conceptual Design Study on LH2 Fueled Supersonic Transport for 2030-35 Time Frame", AIAA-2012-0023, AIAA 50th Aerospace Sciences Meeting, Nashville, USA, Jan. 2012.
- [2] IPCC, URL: http://www.ipcc.ch/publications_and_data/ar4/wg1/en/ch2s2-3-7.html [cited 21 June 2011]
- [3] Grewe, V. et al., "Climate function for the use in multi-disciplinary optimization in the pre-design of supersonic business jet," *The Aeronautical Journal*, Vol.114, No.1154, pp259-269, 2010.
- [4] Grewe, V. and Stenke, A., "AirClim: an efficient tool for climate evaluation of aircraft technology," *Atmospheric Chemistry and Physics*, Vol.8, pp4621-4639, 2008.
- [5] Fonseca, C. M. and Fleming, P. J., "Genetic Algorithms for Multiobjective Optimization: Formulation, Discussion and Generalization," *Proceedings of the 5th international conference on genetic algorithms*, pp. 416-423, 1993.
- [6] Ziemann, J., Mayr, A., Anagnostou, A., Suttrop, F., Lowe, M., Bagheri, S.A. and Nitsche, T., "Potential Use of Hydrogen in Air Propulsion," EQHPP, Phase III.0-3, Final Report, EU, 1998.
- [7] Yoshida, K., "Overview of NAL's Program Including the Aerodynamic Design of the Scaled Supersonic Airplane," held at the VKI, RTO Educational Notes 4, 15-1~16, 1998.
- [8] Carlson, H. W. and Miller, D. S., "Numerical Methods for the Design and Analysis of Wings at Supersonic Speeds," NASA TN D-7731, 1974.
- [9] Glatt, C. R., "WAATS – A Computer Program for Weight Analysis of Advanced Transportation System," NASA CR-2420, 1974.
- [10] Mascitti, V. R., "A Preliminary Study of the Performance and Characteristics of a Supersonic Executive Aircraft," NASA TM-74055, 1977.
- [11] Mack, R. J., "A Supersonic Business-Jet Concept Designed for Low Sonic Boom," NASATM-2003-212435, 2003.
- [12] Fenbert, J. W., Ozoroski, L. P., Geiselhart, K. A., Shields, E. W. and McElroy, M. O., "Concept Development of a Mach 2.4 High-Speed Civil Transport," NASA TP-1999-209694, 1999.
- [13] Robins, A. W., Dollyhigh, S. M., Beissner, F. L. Jr., Geiselhart, K., Martin, G. L., Shields, E. W., Swanson, E. E., Coen, P. G. and Morris, S. J. Jr., "Concept Development of a Mach 3.0 High-Speed Civil Transport," NASA TM-4058, 1988.
- [14] Raymer, D. P., *Aircraft Design: A Conceptual Approach*, 4th ed., American Institute of Aeronautics and Astronautics, Washington, D.C., United States, 2006.
- [15] Mason, M. H., "Software for Aerodynamics and Aircraft Design," URL: http://www.aoe.vt.edu/~mason/Mason_f/MRsoft.html [cited April 2010]
- [16] Public Domain Aeronautical Software, URL: <http://www.pdas.com>. [cited April 2010]
- [17] Seebass, R. and George, A.R., "Sonic Boom Minimization," *Journal of the Acoustical Society of America*, Vol.51, No.2, 1972, pp. 686, 694.
- [18] Darden, C., "Sonic Boom Minimization with Nose-Bluntness Relaxation," NASA TP-1348, 1979.
- [19] Harris, R. Jr., "An Analysis and Correlation of Aircraft Wave Drag," NASA TM X-947, 1964.
- [20] Brewer, G. D., *Hydrogen Aircraft Technology*, CRC, 1990.
- [21] Eshelman, L. J. and Schaffer, J. D., "Real-Coded Genetic Algorithms and Interval-Schemata," *Foundations of Genetic Algorithms 2*, 1993, pp. 187-202.
- [22] Eshelman, L. J., "The CHC adaptive search algorithm: How to have safe search when engaging in nontraditional genetic recombination," *Foundations of Genetic Algorithms*, Morgan Kaufmann Publishers, Inc., San Mateo, 1991, pp. 265-283.
- [23] Tatsukawa, T., Oyama, A. and Fuji, K., "Comparative Study of Data Mining Methods for Aerodynamic Multiobjective Optimizations," *Proceedings of the conference on computational engineering and science*, Vol.13, 2008, pp. 431-434. (in Japanese)
- [24] Kohonen, T., *Self-Organizing Maps*, Springer Series in Information Sciences Springer, Finland, 1994.

**CONCEPTUAL DESIGN STUDY ON LOW BOOM LH2 SUPERSONIC
TRANSPORT – CONSIDERING CLIMATE CHANGE IMPACT-**

- [25] SOMToolbox,
URL:<http://www.cis.hut.fi/somtoolbox/> [cited June 2012]
- [26] NASA, URL:
http://www.aeronautics.nasa.gov/pdf/n3_draft_summary_11_29_07.pdf [cited 10 February 2011]
- [27] Higuchi, K., Zhong, L. and Rinoie, K., "Wing Design of Supersonic Transport by a Multi-Point Optimization Method," ICAS 2008-2.4.3, 26th Congress of International Council of the Aeronautical Sciences, Alaska, USA, Sep., 2008.
- [28] NEDO, "New Energy and Industrial Technology Development Organization, Price of Hydrogen," URL:
<https://app3.infoc.nedo.go.jp/informations/koubo/events/FA/nedoeventpage.2008-06-18.1414722325/> [cited May, 2010, in Japanese]
- [29] EIA, "Spot Prices for Crude Oil and Petroleum Products," URL:
http://www.eia.doe.gov/dnav/pet/pet_pri_spt_s1_d.htm [cited May, 2010]

Table 1 List of property

| | LH ₂ | Kerosene |
|--|-----------------|--------------------|
| Composition | H ₂ | CH _{1.93} |
| Molecular Weight | 2.02 | 168 |
| Energy Density [kJ/g] | 120 | 42.8 |
| Mass Density [kg/m ³] | 71 | 811 |
| Specific Heat [kJ/kg/K] | 9.69 | 1.98 |
| Price[28-29] [US\$/gallon] | 2.4 | 2.2 |

Table 2 Tools utilized

| Tools | Comments |
|-----------------|-------------------------------------|
| WARP | Design wing camber and twist |
| FRICTION | Evaluate frictional drag |
| D2500 | Evaluate wave drag due to volume |
| PANAIR | 3D panel method |
| SEEB | Generate the target equivalent area |

Table 3 LH₂ vs. Kerosene (Initial model)

| | LH ₂ | Kerosene |
|---|-----------------|----------|
| W/S at T/O [psf] | 49.3 | 90.9 |
| T/W at T/O | 0.320 | 0.320 |
| C_L cruise | 0.105 | 0.100 |
| Ave. Altitude [ft] | 51,000 | 42,000 |
| Length [ft] | 479 | 286 |
| Diameter [ft] | 19.2 | 15.1 |
| Fineness Ratio | 25 | 19 |
| Fuselage Volume [ft ³] | 58,000. | 25,000. |
| Wing area [ft ²] | 8,500 | 6,800 |
| W_E [lb] | 289,000 | 229,000 |
| W_F [lb] | 111,000 | 366,000 |
| W_{TO} [lb] | 424,000 | 618,000 |
| L/D | 7.29 | 6.99 |
| Range [nm] | 5,300 | 5,300 |
| ΔT_{CO2} [mK] | 0.00 | 0.68 |
| ΔT_{H2O} [mK] | 2.17 | 0.32 |
| ΔT_{O3} [mK] | 0.24 | 1.15 |
| ΔT_{CH4} [mK] | -0.04 | -0.15 |
| ΔT [mK] | 2.37 | 2.00 |

Table 4 Algorithm settings and optimization conditions

| | |
|-----------------------------|----------------|
| Coding: | Real |
| Fitness: | Pareto ranking |
| Niching: | Sharing |
| Generational change: | CHC |
| Selection: | Random |
| Crossover | BLX-0.5 |
| Mutation | 0% |
| Generation: | 30 |
| Population: | 100 |

Table 5 Design variable ranges and objective functions

| | <i>AR</i> | <i>KINK</i> | <i>LLE1</i> | <i>LLE2</i> | <i>LTE1</i> | <i>LTE2</i> | <i>AREA</i> | <i>FINE</i> | <i>ALT</i> | <i>W_{TO}</i> | <i>L/D</i> | ΔT |
|--------------------|-----------|-------------|-------------|-------------|-------------|-------------|--------------------|-------------|------------|-----------------------|-------------|-------------|
| Unit | - | - | [deg] | [deg] | [deg] | [deg] | [ft ²] | - | [ft] | [lb] | [-] | [mK] |
| Lower limit | 1.50 | 0.30 | 50.0 | 50.0 | -20.0 | 25.0 | 10000 | 18.0 | 50000 | <i>Min.</i> | <i>Max.</i> | <i>Min.</i> |
| Upper limit | 4.00 | 0.80 | 80.0 | 80.0 | 20.0 | 50.0 | 14000 | 24.0 | 65000 | | | |

Table 6 Constrained conditions

| | <i>K@T/O</i> | $\Delta X_{AC@cruise}$ | ΔA_E | <i>Fus. Vol.</i> | <i>Fuel weight</i> | <i>Win. back end</i> | <i>T/W</i> |
|------------------|--------------|------------------------|--------------|------------------|--------------------|----------------------|------------|
| Unit | [-] | [%mac] | [-] | [lb] | [lb] | [%L] | [-] |
| Condition | < 0.22 | < 20 | < 0.06 | 55000 | 100000 | 90 | 0.32 |

Table 7 Average and standard deviation

(a) "Non-pareto solutions"

| | <i>AR</i> | <i>KINK</i> | <i>LLE1</i> | <i>LLE2</i> | <i>LTE1</i> | <i>LTE2</i> | <i>AREA</i> | <i>FINE</i> | <i>ALT</i> | <i>W_{TO}</i> | <i>L/D</i> | ΔT |
|----------------|-----------|-------------|-------------|-------------|-------------|-------------|--------------------|-------------|------------|-----------------------|------------|------------|
| Unit | - | - | [deg] | [deg] | [deg] | [deg] | [ft ²] | - | [ft] | [lb] | [-] | [mK] |
| Ave | 1.67 | 0.58 | 59.7 | 57.2 | 6.6 | 40.5 | 10300 | 20.7 | 54000 | 379000 | 7.74 | 2.41 |
| Stdev | 0.16 | 0.09 | 3.5 | 3.5 | 6.2 | 3.8 | 245 | 0.5 | 790 | 3300 | 0.29 | 0.09 |
| Rate[%] | 9.8 | 15.4 | 5.8 | 6.0 | 93 | 9.3 | 2.4 | 2.6 | 1.5 | 0.9 | 3.9 | 3.6 |

(b) "Pareto solutions"

| | <i>AR</i> | <i>KINK</i> | <i>LLE1</i> | <i>LLE2</i> | <i>LTE1</i> | <i>LTE2</i> | <i>AREA</i> | <i>FINE</i> | <i>ALT</i> | <i>W_{TO}</i> | <i>L/D</i> | ΔT |
|----------------|-----------|-------------|-------------|-------------|-------------|-------------|--------------------|-------------|------------|-----------------------|------------|------------|
| Unit | - | - | [deg] | [deg] | [deg] | [deg] | [ft ²] | - | [ft] | [lb] | [-] | [mK] |
| Ave | 1.59 | 0.58 | 60.7 | 56.6 | 4.5 | 40.5 | 10100 | 20.4 | 54100 | 376000 | 7.85 | 2.38 |
| Stdev | 0.08 | 0.07 | 2.3 | 2.8 | 7.0 | 3.6 | 109 | 0.7 | 1250 | 3100 | 0.23 | 0.11 |
| Rate[%] | 5.0 | 12.6 | 3.8 | 4.9 | 155 | 9.0 | 1.1 | 3.4 | 2.3 | 0.8 | 2.9 | 4.7 |

Table 8 Initial model vs. Optimized model (LH₂)

| | | Initial | Optimized |
|-------------------------------------|--------------------|----------------|------------------|
| <i>W/S</i> at T/O | [psf] | 49.3 | 37.2 |
| <i>T/W</i> at T/O | | 0.320 | 0.32 |
| <i>C_L</i> cruise | | 0.105 | 0.091 |
| Ave. Altitude | [ft] | 51,000 | 54,200 |
| Length | [ft] | 479 | 422 |
| Diameter | [ft] | 19.2 | 20.0 |
| Fineness Ratio | | 25.0 | 21.1 |
| Fuselage Volume | [ft ³] | 58,000. | 55,000 |
| Wing area | [ft ²] | 8,500 | 10,100 |
| <i>W_E</i> | [lb] | 289,000 | 254,000 |
| <i>W_F</i> | [lb] | 111,000 | 100,000 |
| <i>W_{TO}</i> | [lb] | 424,000 | 378,000 |
| <i>L/D</i> | | 7.29 | 7.94 |
| Range | [nm] | 5,300 | 5,870 |
| ΔT_{CO_2} | [mK] | 0.00 | 0.00 |
| ΔT_{H_2O} | [mK] | 2.17 | 2.25 |
| ΔT_{O_3} | [mK] | 0.24 | 0.17 |
| ΔT_{CH_4} | [mK] | -0.04 | -0.04 |
| ΔT | [mK] | 2.37 | 2.38 |

CONCEPTUAL DESIGN STUDY ON LOW BOOM LH2 SUPERSONIC TRANSPORT – CONSIDERING CLIMATE CHANGE IMPACT-

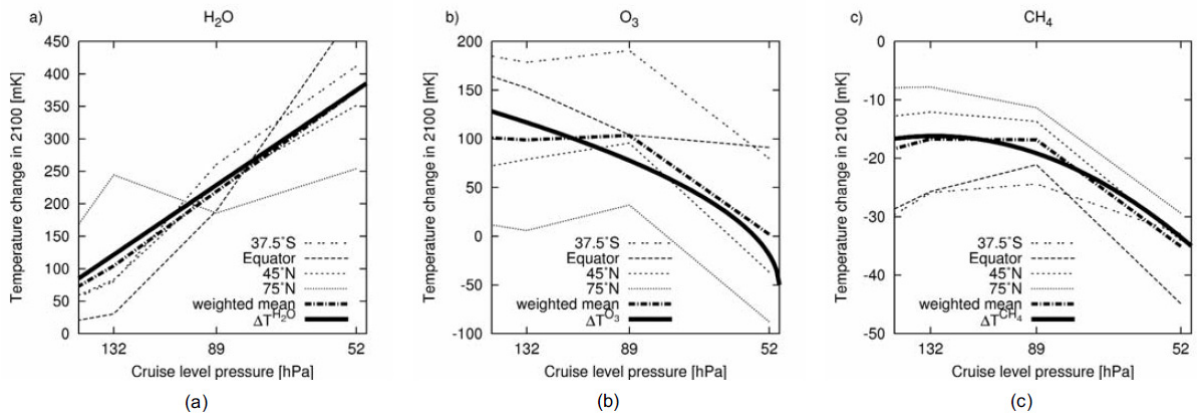


Figure 1 Global mean surface temperature change (ΔT) by H_2O , O_3 and CH_4 [3]

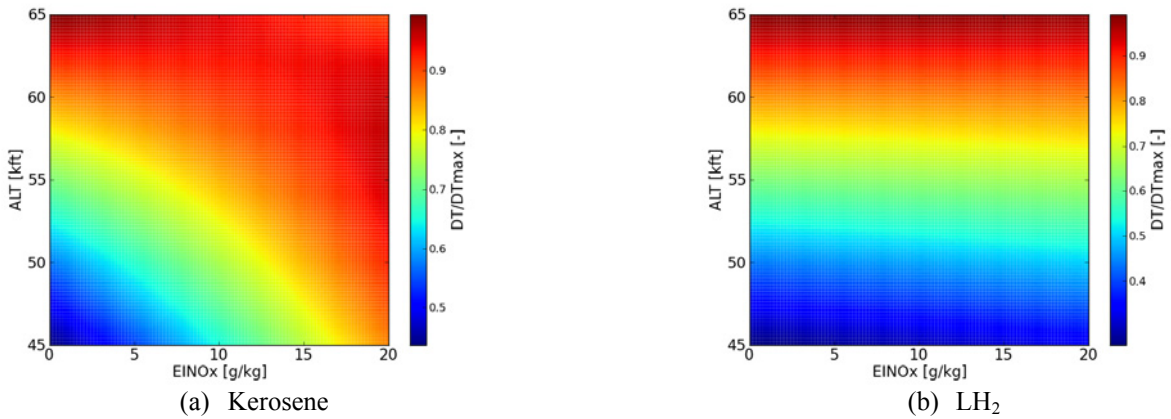


Figure 2 ΔT varied by altitude (ALT) and $EINOx$

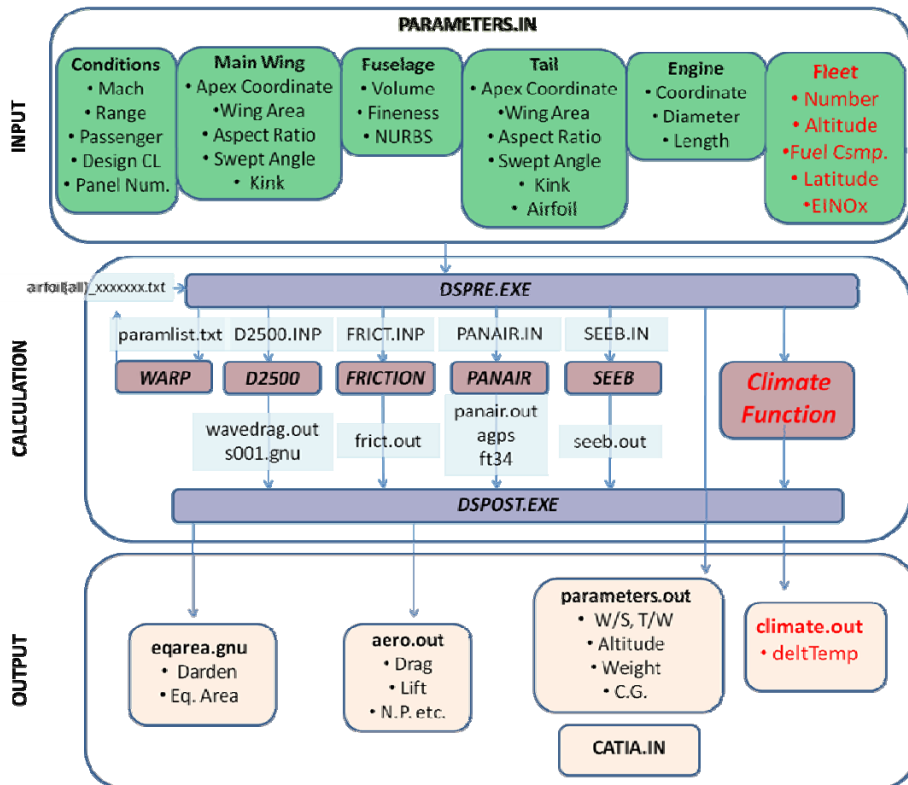


Figure 3 Conceptual design procedure for supersonic transport

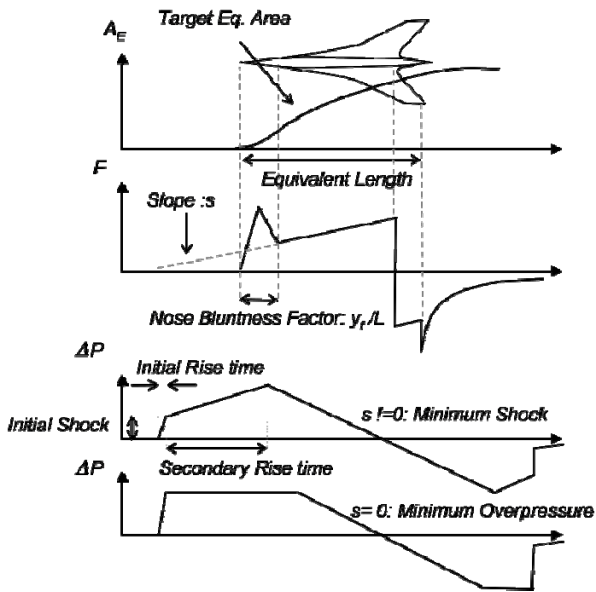


Figure 4 SGD method

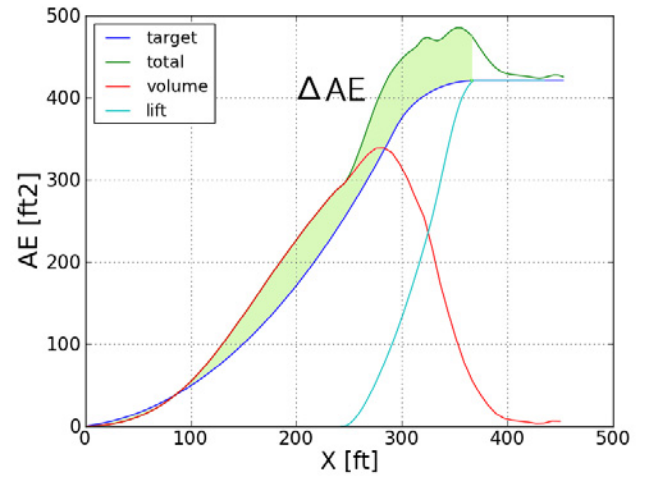


Figure 5 Equivalent area distribution and ΔA_E

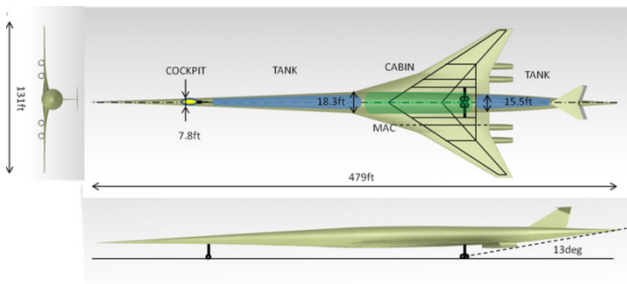


Figure 6 Initial model

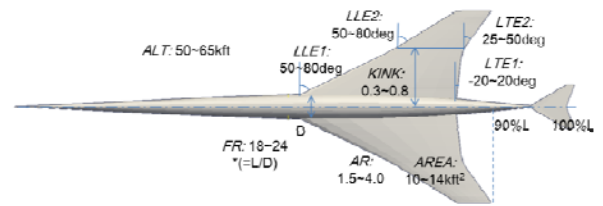
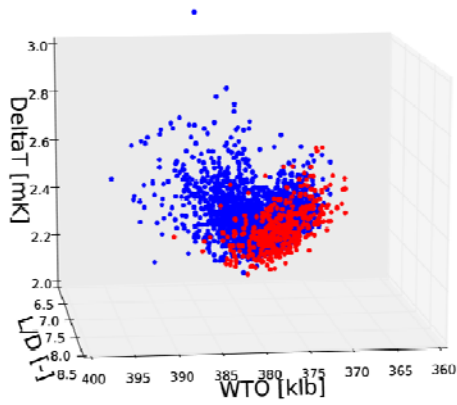
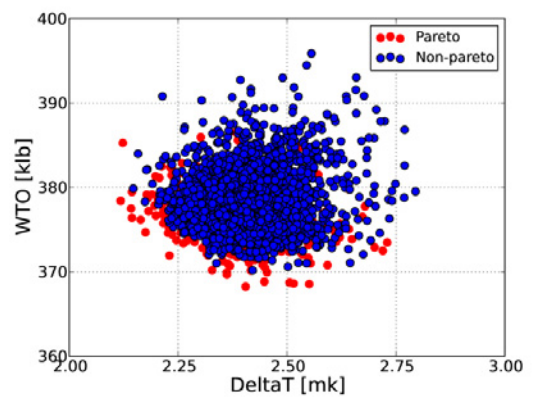


Figure 7 Design variables



(a) Solutions in 3D



(c) W_{TO} vs. ΔT

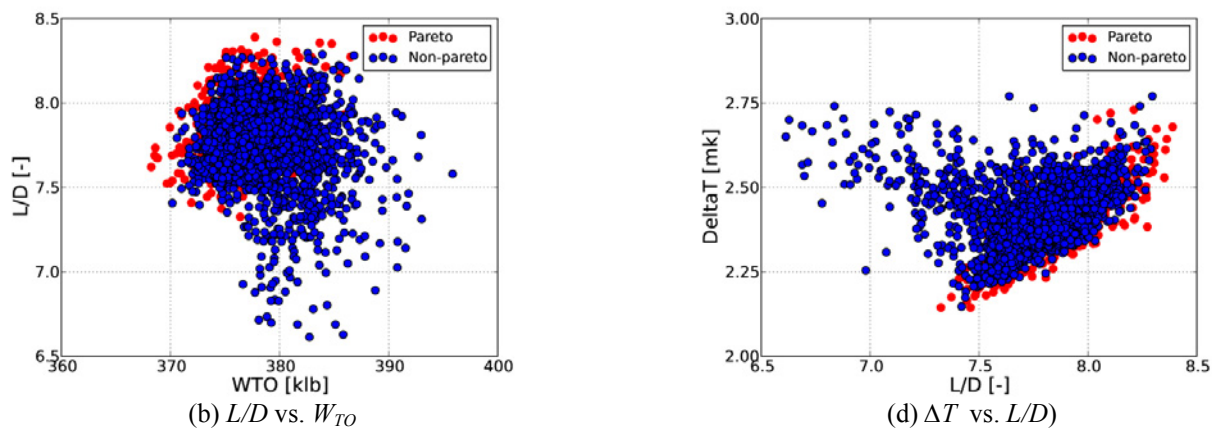


Figure 8 Solutions in 2D and 3D space

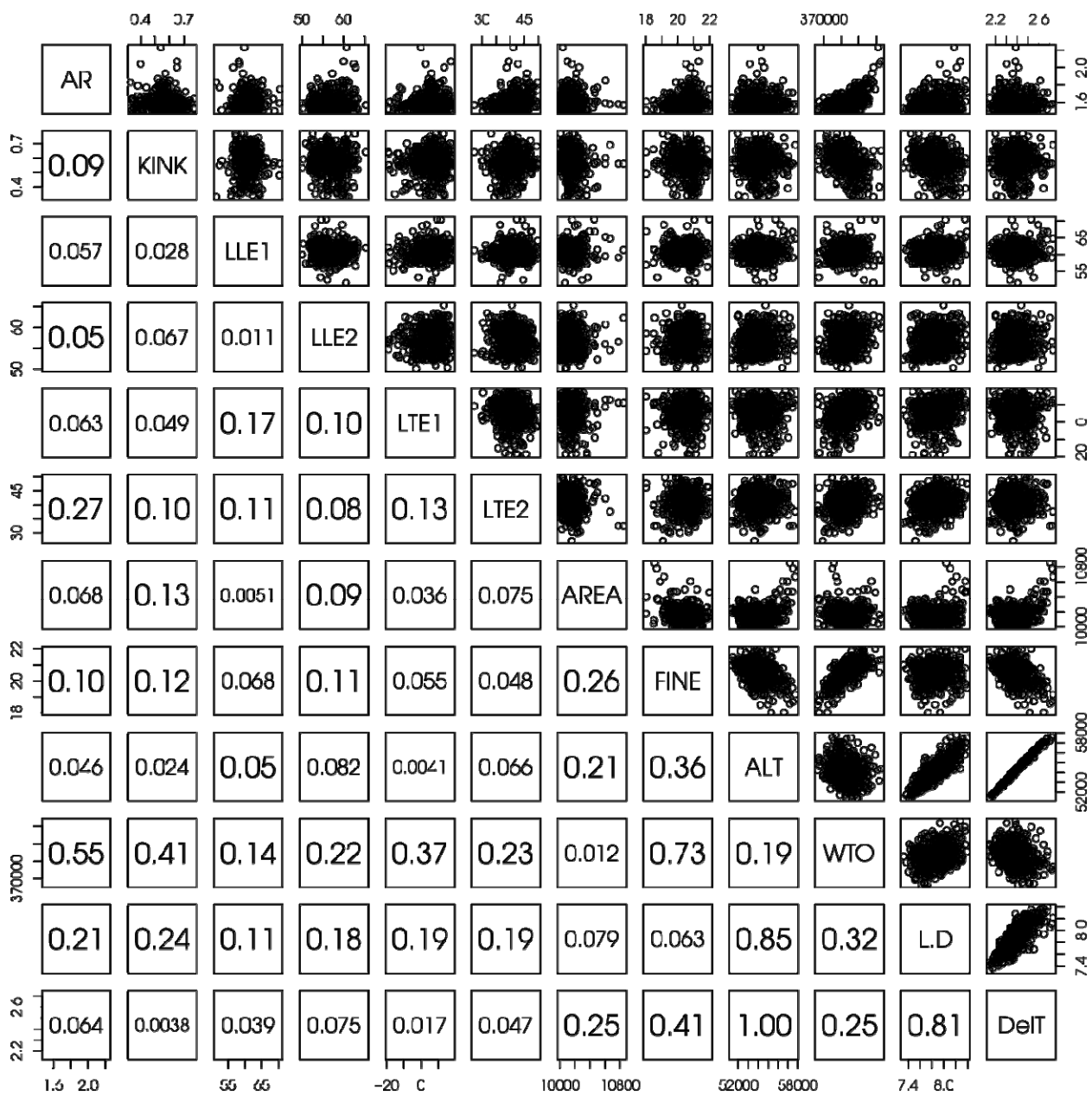


Figure 9 SPM of Pareto solutions

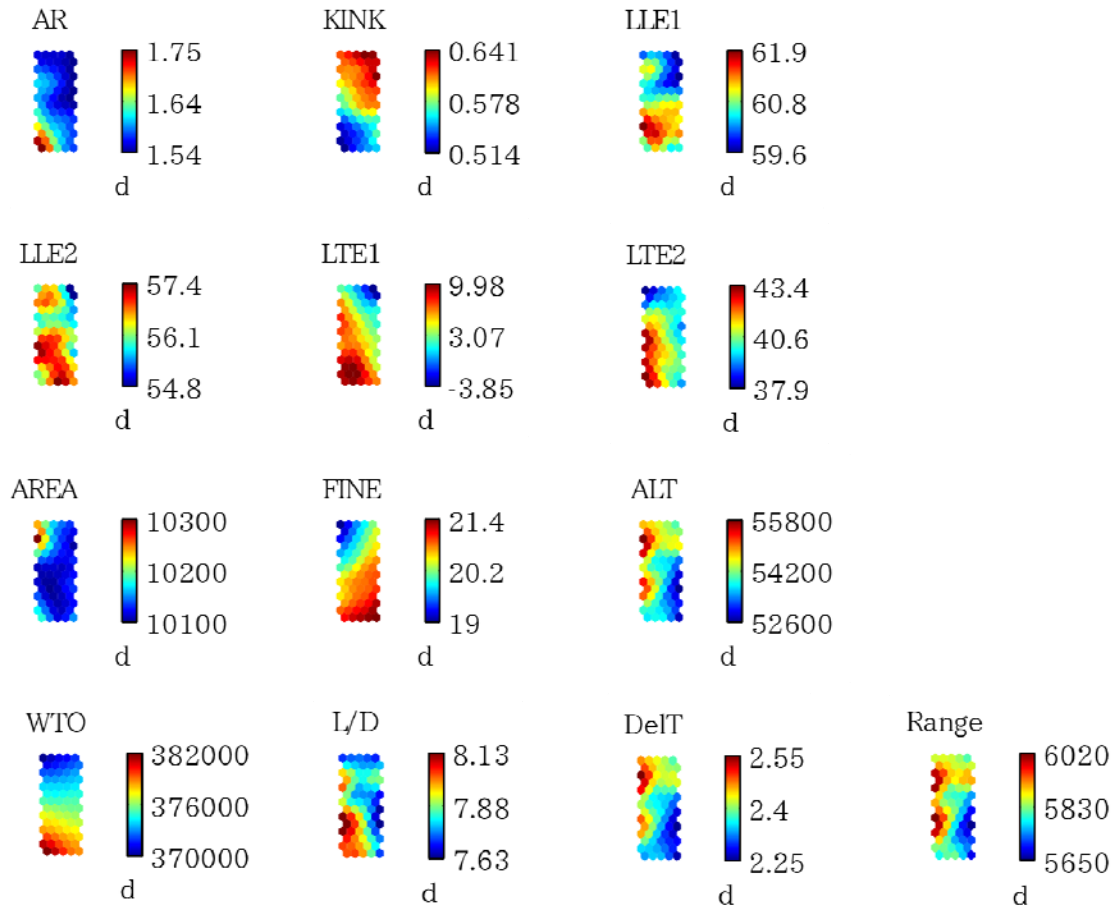
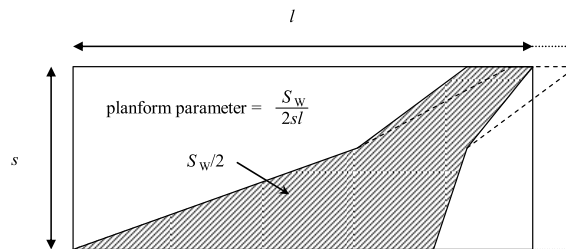
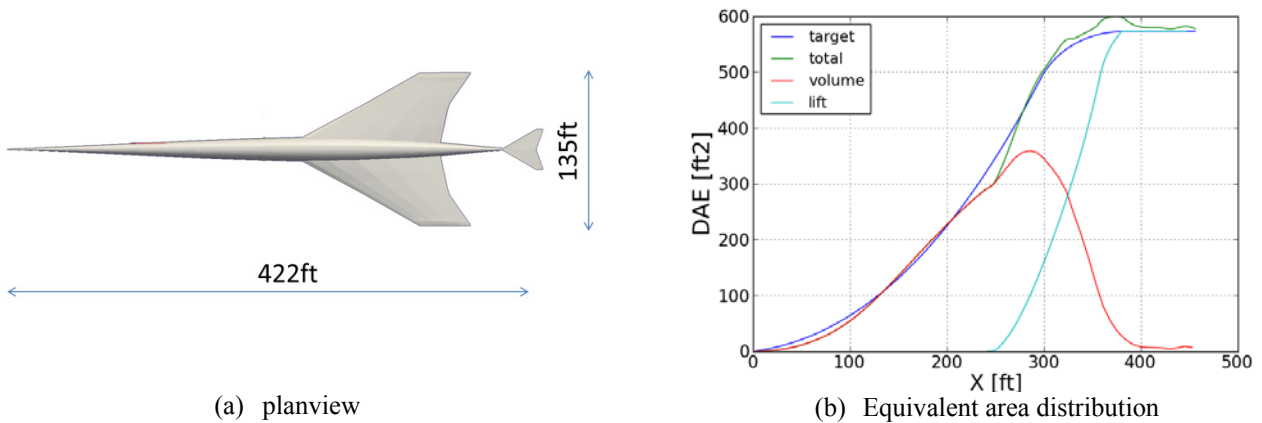


Figure 10 SOM of pareto solutions



* The planform drawn by the dashed line has larger trailing-edge sweep and smaller planform parameter.

Figure 11 Planform parameter [27]



(a) planview

(b) Equivalent area distribution

Figure 12 A population in pareto solutions